Collective Gravity of Minor Planets in the Outer Solar System

Jacob Fleisig

Departmental Honors

Defended on September, 28 2018

Committee:

Thesis Advisor: Dr. Ann-Marie Madigan, Department of Astrophysical and Planetary Sciences,
College of Arts and Sciences Honors Program
Dr. Erica Ellingson, Associate Chair for Undergraduate Studies in the
Department of Astrophysical and Planetary Sciences
Dr. Nan Goodman, Director of the Program in Jewish Studies

Draft version November 5, 2018
Typeset using LaTeX **twocolumn** style in AASTeX62

ABSTRACT

Our Solar System contains a large population of icy bodies beyond the orbit of Neptune. This group of objects, known as the Kuiper Belt, are remnants from early in the formation of the Solar System. However, these bodies exhibit strange orbital characteristics, hinting at the possibility of a missing chapter in the Solar System's formation history. To find an explanation to these phenomena, we investigate the effects that the KBOs' collective gravity has on the Solar System using computer simulations. In doing so, we find a new mechanism capable of changing objects' distances of closest approach to the Sun. We make this new mechanism the main subject of our investigation given that orbits in the Kuiper Belt exhibit strikingly similar attributes. We find that although this new mechanism is thoroughly interesting, it cannot change KBOs' orbits within the age of the Solar System. It could however be responsible for phenomenon a bit farther from home; namely, feeding supermassive black holes and polluting the surfaces of white dwarf stars.

Keywords: celestial mechanics – Outer Solar System: secular dynamics – Kuiper Belt Objects

1. INTRODUCTION

Our Solar System contains a large population of icy bodies beyond the orbit of Neptune. These bodies exist in a cold disk called the Kuiper Belt, located at $\sim 30-50$ AU from the Sun (1 AU is the distance from the Earth to the Sun). Extending away from the Kuiper Belt is the Scattered Disk which can contain orbits at hundreds of AU. The Scattered Disk consists of bodies that made their way to the outer Solar System through scattering interactions with Neptune. The orbits of some of these bodies tilt and cluster together in bizarre ways (Trujillo & Sheppard 2014) that do not conform to the typical story of our Solar System's evolution. The Solar System began as a flat disk of gas and dust, meaning most of the orbits we observe today should also be flat and undisturbed. These new observations of unusual orbits demand an explanation.

Madigan & McCourt (2016) recently found that these bodies are vulnerable to a collective gravitational instability which can explain the observed phenomena. Using computer simulations, they have demonstrated that this "inclination instability" can reproduce much of what we see in the outer Solar System. However, another popular explanation attributes the oddities observed in the outer Solar System to a new Neptune-sized planet, Planet 9 (Brown & Batygin 2016). However, such a planet has yet to be detected!

The simulations performed by Madigan & McCourt (2016) adopt the simple case where all of the Kuiper Belt Objects (KBOs) have the same mass. We want to improve upon these simple simulations and so **we simulate the instability in disks where the bodies are of different masses**. Such mass differences will be present in any realistic setting, such as the outer Solar System, making them important to include. We find that the instability still takes off and, interestingly (in terms of making predictions for the outer Solar System), more massive bodies tend to reach lower inclinations than less massive bodies. In investigating this however, we discovered a new dynamical mechanism that lowers the eccentricity and lifts the periapse distance of massive bodies.

In this paper, we focus mostly on this new mechanism. We are motivated by recent observations of a new population of bodies belonging to a region outside of the Scattered Disk (Gladman et al. 2001). These objects have periapse distances much greater than the semi-major axis of Neptune which implies they have a dynamical history different from that of the Scattered Disk Objects (SDOs) and are *detached* from the inner Solar System. Other histories for these bodies include undergoing evolution in their orbits from interactions with passing stars (Ida et al. 2000) or the hypothetical Planet 9 (Brown & Batygin 2016).

We present our work in the following manner: In section 2 we review the properties of orbits (known as the Kepler elements), define some relevant dynamical processes, and describe the inclination instability. In section 3 we present the effects a large mass has on a disk that undergoes the inclination instability and describe this new dynamical mechanism with idealized N-body simulations. In section 4, we present the results of N-body simulations in increasingly complex/realistic scenarios. We discuss the physics underpinning the mechanism and its relevance in sections 5 & 6. We conclude and examine its implications in section 7.

2. BACKGROUND

In this section, we define dynamical terms which will be useful in later sections.

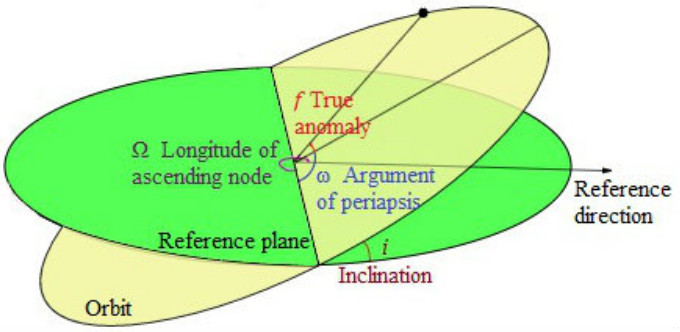

Figure 1. A Visual Representation of the Kepler Elements Four of the Kepler elements are represented in this figure. Inclination (i), the tilt of an orbit, is shown in red on the bottom of the figure. Above that is argument of periapse (ω) in blue. True anomaly (f), the location of the body along its orbit, is shown at the top of the figure in red. Longitude of ascending node (Ω), which describes where the body comes up through the reference plane, is illustrated in the middle of the figure (image credit: http://inspirehep.net/record/1489981/plots).

2.1. *The Kepler Elements*

Kepler elements are used to describe an orbit oriented in 3-D space. With just six numbers, one can describe the shape of an orbit, its size, how its oriented and where a body would be located on such an orbit (see Figure 1). In general, all celestial bodies orbiting a central mass move in ellipses. The Kepler element eccentricity (e) is used to denote how elliptical an orbit is and can range from 0-1. The orbits of planets have near circular orbits with very low eccentricities, i.e. $e \sim 0$, but comets and other bodies have $e \sim 0.6 - 0.9$ (meaning their orbits are elongated). A body's semi-major axis (a) is half the width of its longest axis. For the Earth, which is in a near circular orbit, this value is the distance the Earth is from the Sun (1 AU). Another Kepler element is the inclination (i) or tilt of an orbit. If you were to grab an orbit's *periapse*, the point of the orbit where the body is closest to the central mass, and tilt it off a flat plane, you would be raising its inclination. Now, if you were to instead drag this orbit by its periapse and rotate it about the central mass, you would be changing its argument of periapse (ω). More technically, this is the orientation of the ellipse in the orbital plane. The last two elements we have to describe a body and its orbit are its longitude of ascending node (Ω) and its true anomaly (f). Ω describes where an orbit passes through the "reference frame". The reference frame is represented in the figure as the flat plane which the orbits are oriented with respect to. Lastly, f is the true anomaly; this is where the body is located on its orbit, which can be denoted as the angular separation from its periapse location.

2.2. *Additional dynamical explanations*

Angular momentum and torque

Angular momentum is the rotational equivalent of *linear* momentum. Linear momentum is the mass of an object times its velocity (mv). A car traveling on a straight motorway has strictly linear momentum, but if it were to curve around a winding motorway it would have angular momentum. Celestial bodies orbiting about a central mass also have angular momentum. Their *orbital* angular momentum can be written as

$$J = mr \times v = mJ_c \sqrt{1 - e^2} \tag{1}$$

where r is radial distance from the central mass and $J_c = \sqrt{GMa}$. J_c is the circular angular momentum, or the angular momentum the body would obtain if its orbit was a perfect circle.

Torque, like angular momentum, is the rotational equivalent of a linear quantity. Specifically, a torque is the rotational analog to a force ($\tau = J' = mr \times f$). Unless one enacts an outside torque on a system, angular momentum is conserved. For instance, a skater spins faster with her arms pulled close due to angular momentum conservation. Other physical systems, like the Solar System, behave the same way. Unless another star comes along and drastically disturbs our home, the whole system will contain the same amount of angular momentum it started with. Objects in the Solar System (asteroids, planets, etc.) can distribute angular momentum between themselves, but the total amount must remain constant.

Two-body versus secular dynamics

Bodies can exchange angular momentum through two-body interactions and secular torques. Two-body interactions occur through the mutual scattering of bodies off of each other. Bodies essentially act like gravitational slingshots that change the angular momentum and trajectories of other nearby objects. Secular dynamics is different. Secular torques are *orbit averaged* torques. Imagine spreading an asteroid out along its orbit. The asteroid would now exist as a massive wire which could exert gravitational forces, or torques, on the other wires around it. Torques resulting from these orbit averaged, secular effects are distinctly different from two-body interactions.

Apsidal precession

Apsidal precession is another way to change a body's orbit. Imagine a Solar System with one lone asteroid. This asteroid, if left on its own, would move along the same orbit for billions of years. However, if we were to add thousands more asteroids around the central star, our original asteroid would feel the collective forces from all the others. As a result, its orbit and all the others would rotate like hands on a clock about the central star. This rotation of the asteroid's periapse is apsidal precession.

Dynamical friction

Dynamical friction can also change an object's orbit. Picture a massive billiards ball plowing through a sea of small rubber balls. The billiards ball would lose energy through

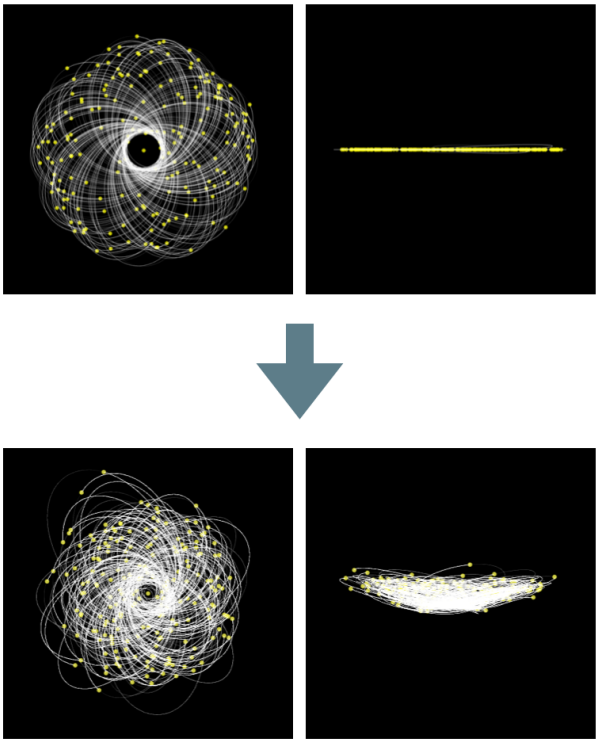

Figure 2. A Visualization of the Inclination Instability Bodies initiated on flat eccentric orbits are vulnerable to the inclination instability. Gravitational torques between the orbits force all the bodies to incline off the initial disk plane (created by graduate student Alexander Zderic, CU Boulder).

drag while, on average, the rubber balls would gain energy from the collisions. This also happens in celestial systems. In stellar clusters, the most massive stars lose energy through *gravitational* drag and sink closer towards the center of the cluster. The less massive stars gain a bit of energy and move outward.

The inclination instability

The inclination instability refers to yet another dynamical mechanism. It is a gravitational instability that occurs in disks of bodies that are on very eccentric ($e > 0.6$) orbits around a central mass. Due to the secular torques the orbits exert on one another, they incline exponentially fast off the mid-plane, drop in eccentricity, and cluster in ω. The latter means that all the orbits tilt in the same way with respect to the mid-plane of the Solar System. Figure 2 is a visual from a computer simulation of the inclination instability. Bodies are initiated on flat orbits and, at later times, incline off the initial disk plane.

3. *N*-BODY SIMULATIONS

Here we explore the inclination instability using `REBOUND` *N*-Body simulations with the IAS15 integrator (Rein & Liu 2012; Rein & Spiegel 2015). *N*-Body simulations are computer programs which calculate the gravitational interactions of particles in a "virtual box" and predict their motions. The simulations in Madigan & McCourt (2016) and Madigan et al. (2018) consider the simplified case where all the disk bodies have the same mass. We improve upon this by simulating the instability in disks where the bodies are of different masses. We start simply: we populate a thin ($i = 10^{-4}$ radians) axisymmetric disk with $n = 400$ bodies all with the same orbital eccentricity, for a variety of starting eccentricities ($e = 0.50$, $e = 0.55$, $e = 0.60$, $e = 0.70$, and $e = 0.80$). We give 399 of them the same mass, m, and let just one other have mass $M = 100m$. We emplace the massive body at semi-major axis, $a_M = 1.0$ and carry out our simulations for 4000 orbital periods at $a = 1$. The mass of the disk is $M_{disk} = 399m + M = 10^{-3}M_*$. We distribute the smaller masses in semi-major axis space uniformly between $0.9 \leq a \leq 1.1$. We choose these high masses to observe the instability quickly in our simulations; since the secular timescale is $t_{sec} \approx (M_*/M)\, P$. We are also limited by computation time to small-n simulations considering the time required for calculations grows significantly with an increasing number of particles. Since we are limited in how many bodies we can simulate, our goal then is to examine the behavior of these low-n disks and extrapolate to high-n systems.

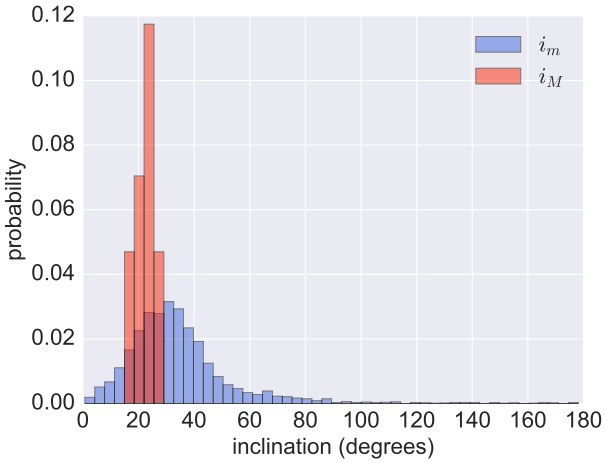

Figure 3. Inclination Distributions for the Large and Small Mass Particles The Gaussian inclination distributions for the large and small mass particles are plotted above. The two bodies' inclination distributions do differ slightly; the more massive bodies tend to have lower inclination values than their less massive counterparts.

3.1. *Effects of different masses on the Inclination Instability*

We find that the presence of a massive body does not disrupt the coherence of the inclination instability, but massive bodies do tend to have lower inclinations after it has acted on the system. Figure 3 illustrates the inclination distributions of

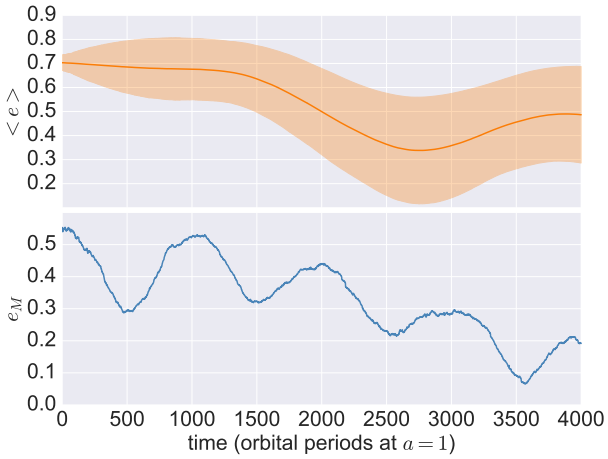

Figure 4. Eccentricity vs. Time (Ideal Simulations) Top Panel: average eccentricity versus time, simulations with no massive body; as bodies' inclinations rise their eccentricities plummet to conserve their z-components of angular momenta. Bottom panel: eccentricity of a massive body versus time, simulations with a massive body; a new mechanism comes to light that becomes the dominant force that shapes the massive body's eccentricity.

the massive and less massive particles. After performing a standard t-test on inclination values obtained after the passage of the instability and obtaining a p-value of 4.56×10^{-8}, we conclude that the massive bodies' and smaller bodies' inclinations are drawn from different distributions and that $\overline{i_M} < \overline{i_m}$. Such a conclusion may be relevant for the outer Solar System as it could be an indication that it has undergone the inclination instability. If observers find that massive bodies in the Kuiper Belt are at consistently lower inclinations than their less massive counterparts, this would be evidence that inclination instability has taken place. Future discoveries of minor planets will enable us to be more certain as to whether this persists in the real Solar System.

3.2. *A New Dynamical Mechanism Takes Form*

Upon further analysis of the behavior of the massive bodies' eccentricities' we find that they undergo oscillatory behavior. This is not a result of the inclination instability but is instead the signature of a new dynamical mechanism. The top panel of Figure 4 exhibits key signatures of the inclination instability. The orange curve is produced from a simulation like those ran by Madigan & McCourt (2016), without any mass differences. The sharp downward drop in eccentricity is therefore caused by conservation of specific angular momentum. As the bodies' inclinations increase, their eccentricities decrease to conserve their z-components of specific angular momentum. However, when we add a massive body, lower the starting eccentricities, and take the disks out of the inclination instability's unstable regime ($e < 0.60$), the new dynamical mechanism becomes

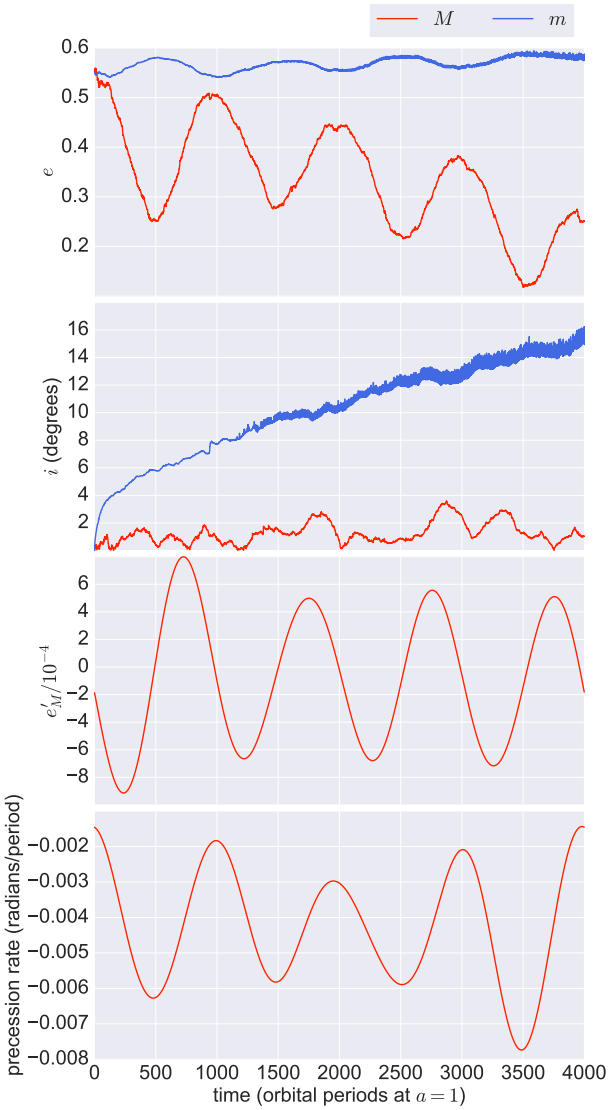

Figure 5. Orbital Elements, Eccentricity Change and Precession Rate vs. Time (Ideal Simulations, $e = 0.55$**)** The massive body's orbit undergoes oscillatory behavior in eccentricity through secular gravitational interactions with a disk of less massive bodies (top, red). The smaller masses exhibit the opposite oscillations (top, blue). The massive body experiences negative change in eccentricity (second from bottom) when its precession rate is decreasing (bottom); this is due to the secular torques exerted by the smaller masses that pile up behind its orbit. The reverse happens when the massive body's precession rate increases.

the dominate force that changes the massive body's eccentricity (see bottom of Figure 4). This new dynamical driver that comes to light results from the interaction of two effects: differential apsidal precession and secular gravitational torques between the more and less massive orbits. All the orbits undergo apsidal precession and rotate in retrograde about the xy-plane like the hands on a clock. The more massive object

undergoes slow precession relative to the others. This creates an over-density of orbits on one side of *its* orbit. The smaller masses then donate their angular momentum to the massive body via secular gravitational torques. As a result, the massive body drops its orbital eccentricity, lifts its periapse distance and begins to precess more quickly (see Figure 5). The massive body, now precessing more rapidly, subsequently catches up to the rest of the disk where it can donate its angular momentum back to the sea of less massive particles. Secular torques now act in the opposite direction as before and the massive body increases its orbital eccentricity. Therefore, this mechanism is cyclical and causes oscillatory behavior in the massive body's eccentricity and periapse distance.

We calculate the massive body's precession rate by obtaining the rate of change of its i_e vector. This vector, first introduced by Madigan & McCourt (2016), determines the orientation of an orbit. It is represented by the projection of its eccentricity vector in the xy-plane (i.e. $i_e = \arctan \frac{e_y}{e_x}$). To find the precession rate as a function of time we calculate the numerical derivative of the massive body's i_e value and perform a discrete Fourier transform (DFT), subtracting out high frequency noise components. We do the same once more to obtain the derivative of the massive object's eccentricity (see Figure 5).

The massive body also experiences a net drop in eccentricity over the course of thousands of orbits. This is due to secular effects as well as dynamical friction. The massive body sinks towards the center of the gravitational potential (via two body interactions) where there is less mass present in its orbital annulus. Therefore, the relative precession rates between the massive and less massive bodies become larger and, even though there is less disk mass here, the massive body interacts with a greater *fraction* of the disk than before. These interactions donate a net positive angular momentum to the massive body that cause its eccentricity oscillations to occur around increasingly smaller values.

It is important to note that these eccentricity oscillations are distinctly different from Kozai-Lidov oscillations (Lidov 1962; Kozai 1962). The Kozai-Lidov mechanism refers to eccentricity and inclination oscillations of a satellite caused by perturbations from a significantly more massive body. This is not what occurs in our simulations. Eccentricity oscillations result from the collective gravitational torques between orbits and we see no evidence of inclination oscillations (see Figure 5).

4. N-BODY SIMULATIONS OF INCREASING REALISM

In the previous section, we showed how angular momentum exchange between a large mass body and smaller mass bodies results in eccentricity oscillations in a simplified set-up. But, this mechanism could be applicable to a range of more complex systems. For example, recent observations reveal a

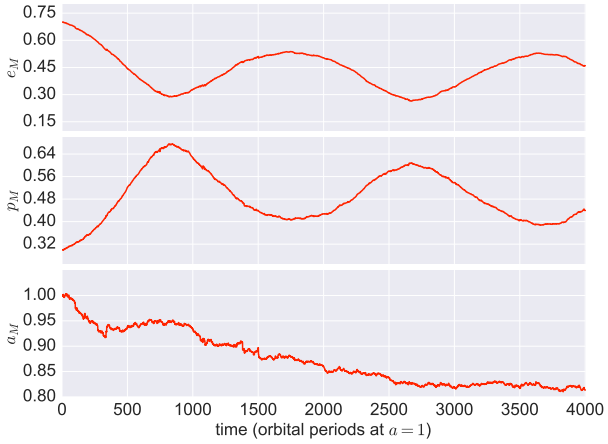

Figure 6. Eccentricity, Periapse, and Semi-Major Axis of the Massive Body vs. Time (Scattered Disk Simulations) The detachment mechanism persists when the bodies are initiated on Scattered Disk orbits. Eccentricity and periapse distance exhibit downward and upward trends respectively, as a result of dynamical friction. The massive body sinks towards the center of the potential where the eccentricity value needed to precess with the rest of the disk decreases.

number of bodies in the Scattered Disk region of our Solar System that have periapse distances much greater than the semi-major axis of Neptune (Gladman et al. 2001). These are called "detached objects". Could the new mechanism we describe be responsible for raising the perihelia of massive Scattered disk objects and thus detaching them? The real Solar System is a messy place. To test this idea, we need to make our simulations less idealized and more realistic. We do this in three steps. First, we initialize all masses on orbits consistent with the Scattered Disk population (explained below). In the second round of simulations, we include impulsive scattering events from Neptune. In the third and final round of additional simulations, we use a distribution of masses. These simulations are written in the same code as the ideal cases, `REBOUND` (Rein & Liu 2012). They are integrated for between 3000 – 8000 orbital periods at $a = 1$ using the IAS15 integrator (Rein & Spiegel 2015). We emplace the massive body, again, at semi-major axis $a_M = 1$.

4.1. *Scattered disk profile*

In this round of simulations, we start the particles on orbits consistent with those observed in the Scattered Disk. The Scattered Disk, first discovered by Luu et al. (1997), is the trans-Neptunian regime in the outer Solar System. Bodies in this region were scattered outward by Neptune in the past and have orbits with periapse distance $\sim$ 30 AU bringing them close to Neptune upon return passages through the inner Solar System. Therefore, the eccentricity of a SDO grows with increasing semi-major axis such that its periapse distance stays

fixed to Neptune. To mirror this pattern in our simulations, we spread out bodies in semi-major axis space between $0.5 \leq a \leq 5.0$ according to a $1/a$ surface-density profile. Our scattered bodies have periapse distances, p, equal to 0.3. Therefore, the assigned e values are dependent on the assigned a values such that $e = 1 - p/a$. We assign inclinations in accordance with a Rayleigh distribution where the mean inclination is 5°.

We find that the detachment mechanism persists when the bodies are initiated on Scattered Disk orbits (see Figure 6). The eccentricity and periapse distance of the massive body undergo upward and downward oscillations respectively. The massive body also experiences a net drop in its eccentricity due to dynamical friction, which we discussed earlier. In short, we conclude that this mechanism is robust for initial conditions that emulate the Scattered Disk.

4.2. *Scattering from Neptune*

In this round of simulations, we subject the particles to continual scattering from a Neptune-like planet. We cannot include Neptune though as an active particle in our simulations due to our chosen values of the disk mass, which we bumped up to observe the secular effects more quickly. If we assume that Neptune has a mass on the order of 10^6 times that of a typical Scattered Disk object, then an active Neptune in our simulations would have mass greater than that of the central star!

To overcome this problem, we include a programmed scattering force in our simulations. The force is added using the `REBOUNDX` library. Duncan et al. (1987) approximated the average change in energy from scattering interactions with Neptune. Figure 1 of their work implies that for a low inclination object with $a \approx 100$ AU, the average change in orbital energy is approximately $< (\Delta x)^2 >^{1/2} = 2.5 \times 10^{-5}$ AU^{-1} (Duncan et al. 1987). The resulting scattering diffusion timescale is $t = 2.5 \times 10^5$ orbital periods. The fractional change in a per orbital period is therefore $< \Delta a > /a = (\Delta t/t)^{1/2}$ which is equivalent to 2×10^{-3}. We subject all the bodies in our simulations to this fractional change in a every periapse passage as long as their periapse distances are $p \leq 0.35$. We change their eccentricities accordingly to keep periapse distances fixed. There is an equal probability that the bodies are scattered inward or outward. Consequently, the objects undergo random walks in energy proportional to their semi-major axes.

We conclude that periodic scattering also does not affect the viability of our detachment mechanism (see Figure 7). As we stated previously, the scattering diffusion timescale for the masses in our simulations is 2.5×10^5 orbital periods. This is the length of time required for a body to experience a change in semi-major axis proportional to its initial a value. Since the secular torques in our simulations change orbits on timescales of $\sim 10^3$ orbital periods, scattering does not change our bodies' semi-major axes quickly enough for them to be diminished. Scattering also does not change the orientation of the orbits, allowing the secular torques to keep acting in the same directions.

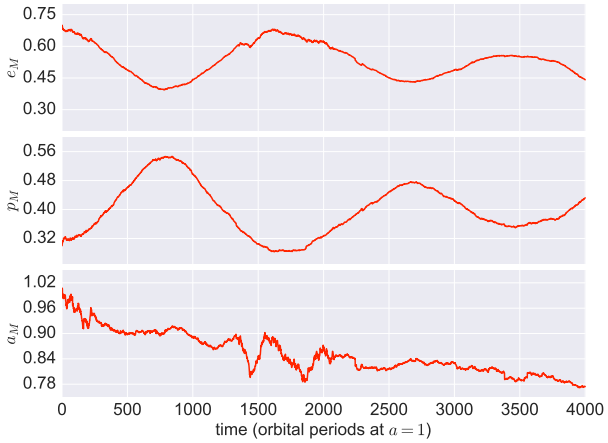

Figure 7. Eccentricity, Periapse, and Semi-Major Axis of the Massive Body vs. Time (Scattering Simulations). The detachment mechanism continues to act on the massive body even in the presence of continual scattering from the giant planets. Bodies are given a kick every periapse passage as long as their periapse distance is $p \leq 0.35$.

4.3. *Distribution of masses*

In our third and final round of additional simulations, we assign masses to our bodies according to a power-law distribution. Using observations and collisional models to probe the histories of KBOs, Kenyon & Bromley (2004) estimated that the number density of KBOs $dN/dr \propto r^{-\alpha}$ where $\alpha \approx 2.5-3.0$ for small bodies (with radii $r \lesssim 0.1 - 1.0$ km) and $\alpha \approx 3.5$ for large bodies (with radii $r \gtrsim 10 - 100$ km). Our aim is not to emulate this exact broken power law in our simulations but to show that this mechanism is robust for a realistic mass distribution. If we assume that $\alpha = 3.0$ and hold the density of the masses constant, then $dN/dm \propto m^{-5/3}$. We assign mass values, according to this density profile, that span six orders of magnitude.

In Figure 8 we show that the mechanism is robust with a mass distribution. The most massive body in these simulations (with mass $M \approx 3 \times 10^{-4}$ such that $M/M_{disk} \approx 0.3$) undergoes the same cyclical orbital changes in eccentricity and periapse. This result is noteworthy because any real physical system, such as a scattered debris disk, would contain a population of bodies with a variety of masses. Additionally, one might argue that the presence of multiple massive bodies may disrupt the coherence of the mechanism. However, we show in these simulations that it still preferentially detaches the most massive bodies.

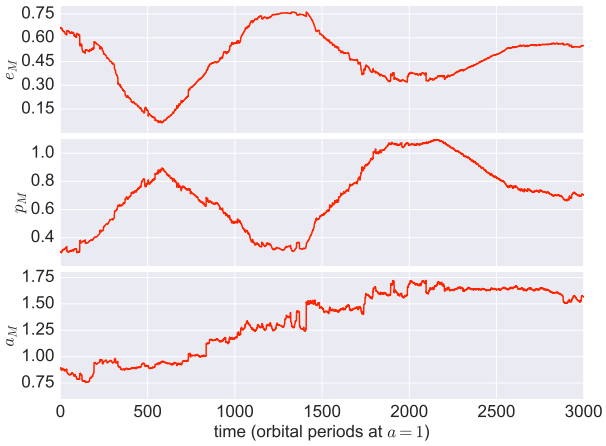

Figure 8. Eccentricity, Periapse, and Semi-Major Axis of the Massive Body vs. Time (Power-law Simulations). The detachment mechanism persists for a realistic mass distribution. We assign masses in accordance with a realistic power law size distribution where $dN/dr \propto r^{-3}$.

5. MECHANISM

In this section, we aim for an analytic description of the physics of the new mechanism. To do so, we consider again the idealized set up of an axisymmetric disk consisting of a large number (n) of small mass bodies (m) on high eccentricity ($e_{m_0} = e_m[t = 0]$) orbits about a central mass M_*. Into this system, we place a single body of higher mass (M) with orbital eccentricity (e_{M_0}). For simplicity, we assume all bodies have the same semi-major axis and orbital plane.

The orbits will apsidally precess due to their mutual gravitational forces. If orbit M precesses at a different rate with respect to the lower mass orbits, it will experience a flow of orbits to one side and exchange angular momentum with them via secular torques. Its precession rate over one orbital period is

$$\Gamma_M \approx \frac{M^*(<a)}{M_*}\sqrt{1-e_{M_0}^2} = \frac{nm}{M_*}\sqrt{1-e_{M_0}^2} \tag{2}$$

(Merritt et al. 2010) while the precession rate of small mass bodies is

$$\Gamma_m \approx \frac{nm+M}{M_*}\sqrt{1-e_{m_0}^2}. \tag{3}$$

Hence if $e_{M_0} = e_{m_0}$, orbit M will precess at a slower rate than orbits m. To precess at the same rate, it will need to decrease its orbital eccentricity (which it will do via the exchange of angular momentum with surrounding orbits).

We calculate this equilibrium eccentricity by setting $\Gamma_{\rm diff} = \Gamma_m - \Gamma_M = 0$, which yields

$$\sqrt{1-e_{\rm eq_M}^2} = \left(\frac{nm+M}{nm}\right)\sqrt{1-e_{m_t}^2}. \tag{4}$$

$e_{\rm eq_M}$ is the eccentricity at which the massive orbit M would precess at the same rate as the lower mass orbits. Note however $e_{m_t} \neq e_{m_0}$. As total angular momentum of the system is conserved, the massive body cannot reach the equilibrium orbital eccentricity without changing the average eccentricity of the surrounding lower mass orbits. Conservation of orbital angular momentum yields

$$J_M + nJ_m = MJ_c\sqrt{1-e_{M_t}^2} + nmJ_c\sqrt{1-e_{m_t}^2} = J_{\rm tot} \tag{5}$$

where $J_c = \sqrt{GM_*a}$ is the circular angular momentum and $J_{\rm tot}$ is the conserved total angular momentum. Combining equations 4 and 5 and taking $e_{M_0} = e_{m_0}$ yields the expression for equilibrium eccentricity

$$\sqrt{1-e_{\rm eq_M}^2} = \delta\sqrt{1-e_{\rm m_0}^2} \tag{6}$$

where

$$\delta = \frac{(1+\alpha)^2}{\alpha^2+(1+\alpha)} \tag{7}$$

and

$$\alpha = \frac{nm}{M}. \tag{8}$$

We calculate the oscillation period by quantifying the time it takes the massive orbit to reach the equilibrium eccentricity via the exchange of angular momentum with surrounding lower mass orbits; this is a quarter of the oscillation period. The change in angular momentum due to torques exerted on orbit M over one orbital period is given by

$$\Delta J_p \approx \frac{\pi}{2}\chi\, e_{m_0}\frac{nm}{M_*}J_c \tag{9}$$

where χ (< 0.5) is the fraction of disk orbits that donates a net positive angular momentum to orbit M, $\beta(e) \approx 0.25e$ is the eccentricity dependent factor that influences the strength of the secular torque (Gürkan & Hopman 2007), and J_c is the body's circular angular momentum. From numerical experiments we find $\chi \approx 0.3$. The oscillation period is then

$$t_{\rm osc} = 8\,(\pi\chi\, e_{\rm m_0})^{-1}\frac{\Delta J}{J_c}\frac{M_*}{nm}P \tag{10}$$

where ΔJ is the change in angular momentum needed to reach the equilibrium eccentricity. We find that the oscillation timescale for our simulations should be $\sim 1.2\times10^3 P$, which is in rough agreement with our numerical results (see Figure 5).

6. RELEVANCE OF MECHANISM TO REAL ASTROPHYSICAL SYSTEMS

6.1. *How (not) to make Detached Objects*

We can now calculate the oscillation timescale for a typical detached object in the Solar System. Sedna, discovered by Brown et al. (2004) is our example case. It has a periapse distance of 76 AU, a semi-major axis of 506 AU, an eccentricity of 0.85, and an orbital period of 11,400 years.

From equation 6, it holds that the lowest equilibrium eccentricity is obtained when δ is at its maximum. This occurs when $nm \sim M$ (see Figure 9). If $M \gg nm$, δ asymptotically approaches unity and $e_{eq_M} \approx e_{M_0} = e_{m_0}$ (since the massive body can only take so much angular momentum from the surrounding orbits). The same occurs when $M \ll nm$. This is because as the disk becomes increasingly massive, the precession rates of all of the Scattered Disk Objects (SDOs) are essentially equivalent and again, $e_{eq_M} \approx e_{M_0}$. Therefore, in order for Sedna to achieve its current eccentricity through this mechanism it must interact with a disk equivalent to its mass (i.e. $nm \sim M$) and its equilibrium eccentricity must be $e_{eq_M} = 0.89$, given that it starts as a member of the Scattered Disk with eccentricity $e_{M_0} = 0.94$. From equation 10 we can calculate Sedna's oscillation timescale, with the assumption that it interacts with a disk of SDOs of similar mass to itself. We find that $t = 3.5 \times 10^{30}$ years!! This indicates that Sedna could not have possibly undergone detachment via this mechanism within the age of the universe (let alone the age of the Solar System).

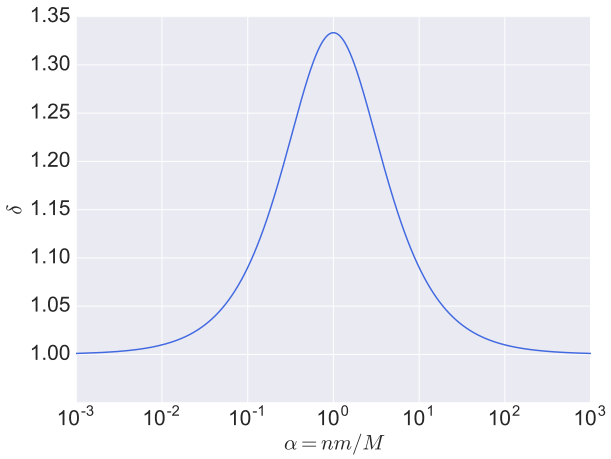

Figure 9. δ vs. Disk Mass δ approaches unity for sufficiently high and low disk masses. Maximum occurs when $nm \sim M$. The lowest equilibrium eccentricity a massive body is allowed to have is determined by maximizing δ.

We conclude that although our simulations demonstrate the robustness of our mechanism in increasingly realistic conditions, it is unfortuneately not relevant to the Scattered Disk. The massive body in our simulations has a mass that is comparable to that of the rest of the disk. Additionally, the mass of the disk is on the order of one Jupiter mass. Since $t_{osc} \propto \frac{M_*}{nm} P$, detachment of massive bodies in our simulations occur within hundreds of orbital periods. Unfortunately, Sedna and the real Scattered Disk have masses nowhere near the value of a Jupiter mass. As a result, it would not be possible for massive SDOs and minor planets to detach from the Scattered Disk through this mechanism.

6.2. *Circularizing Planet 9?*

Could the hypothetical Planet 9 decrease its orbital eccentricity via this mechanism? One formation mechanism for the hypothesized planet is that it was scattered outward by the influence of giant protoplanets beyond the frost-line in the outer Solar System. Thommes et al. (1999) & Levison & Morbidelli (2007) demonstrate how protoplanets similar to Planet 9's predicted mass could be scattered outward while young giants are clearing debris from their orbital domains. If Planet 9 exists and was formed by such processes, it would be challenging to explain its currently low(er) eccentricity; which is predicted to be $\sim 0.5 - 0.8$.

Planet 9 must have a mass of $\sim 5 - 10 M_\oplus$ and a semi-major axis of $\sim$ 700 AU (Batygin & Morbidelli 2017). Using the arguments in the introduction of this section, we maximize δ and minimize the equilibrium eccentricity by hypothesizing that Planet 9 interacts with a disk equivalent to its mass. Assuming that it started in the Scattered Disk with an eccentricity $e_{M_0} = 0.96$, we find its equilibrium eccentricity to be $e_{eq_M} = 0.92$. This value is higher than Planet 9's predicted eccentricity, indicating that Planet 9 could not have reached its current orbit through this mechanism.

6.3. *Where could this mechanism be relevant?*

Although this mechanism is not important in the outer Solar System, it could be for other Keplerian systems which host disks of sufficiently high mass (i.e. $M_{disk} \sim 10^{-3} M_*$) and contain a distribution of bodies in which the most massive objects differ in mass from their average counterpart by a factor of $\sim$ 100 or more. For example, disks containing stars and intermediate mass black holes (IMBHs) in orbit about super massive black holes (SMBHs) could preferentially circularize the most massive bodies while feeding the central SMBH with IMBHs or stars. This is important, considering that an open question among astrophysicists is how to continually feed SMBHs. Additionally, it is known that many white dwarfs have surfaces polluted heavily by metals (Cottrell & Greenstein 1980). It is unclear how such stars could accumulate metallic surfaces, but one suggestion is a continuous bombardment of asteroids from a planetesimal disk. A massive planet ($\sim M_{Jup}$) embedded in a planetesimal disk roughly equal to its mass could circularize its orbit through this new mechanism and, in the process, generate a flux of bodies that reach high enough eccentricities such that they interact with the central white dwarf on timescales of $\sim 10^4$ years. Please see the Appendix (section 7) for more details on this phenomenon.

7. SUMMARY AND DISCUSSION

In this paper we have shown that in a thin axisymmetric disk of eccentric orbits, massive bodies precess at slower rates than their less massive counterparts. Smaller masses orbits pile up to one side of a massive body's orbit and donate their angular momentum via secular gravitational torques. As a result, massive bodies undergo oscillatory behavior in eccentricity and periapse in an effort to obtain an equilibrium precession rate consistent with the rest of the disk.

Using N-body simulations of increasing realism, we find that this mechanism is robust in outer Solar System conditions. These conditions are, namely, eccentricities and semi-major axes consistent with the Scattered Disk population, scattering forces from the giant planets/stars, and a distribution of masses that follow a $m^{-5/3}$ power law. Sadly, this mechanism is not capable of detaching Sedna from the Scattered Disk given that the timescale to do so is 3.7×10^{30} years if the mass of the Scattered Disk in its vicinity is on the order of its own mass. Thus, this mechanism, although interesting (and new!), is not capable of detaching massive minor planets in the Trans-Neptunian region. However, this mechanism could be important for exoplanet systems hosting Jupiter mass planets embedded in planetesimal debris disks. It could also have implications for polluted white dwarfs and the feeding of SMBHs.

REFERENCES

Batygin, K., & Morbidelli, A. 2017, AJ, 154, 229

Brown, M. E., & Batygin, K. 2016, ApJ, 824, L23

Brown, M. E., Trujillo, C., & Rabinowitz, D. 2004, The Astrophysical Journal, 617, 645

Cottrell, P. L., & Greenstein, J. L. 1980, ApJ, 242, 195

Duncan, M., Quinn, T., & Tremaine, S. 1987, AJ, 94, 1330

Gladman, B., Kavelaars, J. J., Petit, J.-M., et al. 2001, AJ, 122, 1051

Gürkan, M. A., & Hopman, C. 2007, MNRAS, 379, 1083

Hills, J. G. 1981, AJ, 86, 1730

Ida, S., Larwood, J., & Burkert, A. 2000, ApJ, 528, 351

Kenyon, S. J., & Bromley, B. C. 2004, The Astronomical Journal, 128, 1916

Kozai, Y. 1962, AJ, 67, 591

Levison, H. F., & Morbidelli, A. 2007, Icarus, 189, 196

Li, G., Naoz, S., Kocsis, B., & Loeb, A. 2014, ApJ, 785, 116

Lidov, M. 1962, Planetary and Space Science, 9, 719

Luu, J., Marsden, B. G., Jewitt, D., et al. 1997, Nature, 387, 573

Madigan, A.-M., Halle, A., Moody, M., et al. 2018, ApJ, 853, 141

Madigan, A.-M., & McCourt, M. 2016, MNRAS, 457, L89

Merritt, D., Alexander, T., Mikkola, S., & Will, C. M. 2010, Phys. Rev. D, 81, 062002

Rein, H., & Liu, S.-F. 2012, A&A, 537, A128

Rein, H., & Spiegel, D. S. 2015, MNRAS, 446, 1424

Thommes, E. W., Duncan, M. J., & Levison, H. F. 1999, Nature, 402, 635

Trujillo, C. A., & Sheppard, S. S. 2014, Nature, 507, 471

APPENDIX

7.1. *Comet Showers*

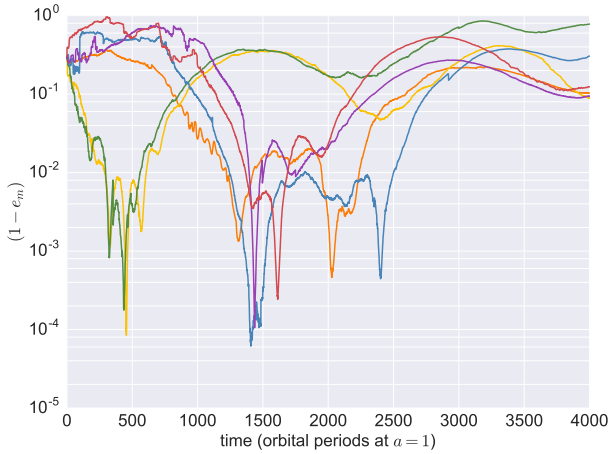

Figure 10. Eccentricity Evolution of small Masses in ideal simulations with initial eccentricity $e = 0.70$ Small masses undergo eccentricity oscillations, similar to those of the massive body but in opposite direction and of higher amplitude. As eccentricities grow the small bodies are in danger of colliding with the central object at periapse.

The angular momentum exchange between large and small mass bodies can generate an influx of small masses into the center of the gravitational potential. As the more massive body is torqued to low eccentricities, the reverse happens to the smaller masses (Figures 5 & 10). As a result, some are kicked to very high orbital eccentricities, $e \approx 0.999$, and they are in danger of colliding with the central star (or even terrestrial planets).

7.2. *Retrograde Orbiters*

Our simulations also produce retrograde orbiters. This occurs when the small masses are torqued to high enough eccentricities such that they undergo "inclination flips" (Li et al. 2014). This refers to a body whose orbit has been torqued so greatly that its inclination goes through a 180° flip, causing the body to circle the sun backwards! This occurs in our simulations due to the artificially high masses of our particles (which are chosen for computational simplicity). Particles take steps in angular momentum greater than that of the Sun's loss cone and survive. Essentially, these bodies exist in the full loss cone regime (Hills 1981). This regime is defined by a large ratio between the size of a comet's jump in angular momentum per orbital period to that of the loss cone , $q >> 1$, where

$$q = \left(\frac{\Delta J_p}{J_{LC}}\right)^2. \tag{11}$$

The angular momentum of the loss cone is

$$J_{LC} = \sqrt{2GM_\odot R_\odot}. \tag{12}$$

ΔJ_p is the change in angular momentum per orbital period given by equation 9. Again, $\Delta J_p \approx 2\pi\,\chi\,\beta(e)\,\frac{nm}{M_\odot}\,J_c$ where χ (< 0.5) is the fraction of disk orbits that donates a net positive angular momentum to orbit M, $\beta(e) \approx 0.25e$ is the eccentricity dependent factor that influences the strength of the secular torque (Gürkan & Hopman 2007), and J_c is the body's circular angular momentum. From numerical experiments we find $\chi \approx 0.3$. In the real Solar System, the size of the Sun's loss cone relative to a comets typical jump in angular momentum is therefore

$$q = \left(\frac{nm\,\pi\,\chi\,\beta(e)}{M_\odot}\right)^2 \left(\frac{a}{R_\odot}\right) \sim 10^{-8}. \tag{13}$$

This indicates that the bodies' periapse distances would cross through the radius of the Sun, i.e., these bodies would collide with the Sun, and they would not become retrograde orbiters.